e-ISSN: 2722-9807

Sriwijaya Journal of Ophthalmology

[SJO]

https://sriwijayaophthalmology.com

Retinal Microvascular Changes on OCT-Angiography in Preclinical Alzheimer's Disease: A Prospective Indonesian Cohort Study

Taufiq Indera Jayadi[1], Eva Naritawati[1*], Akmal Hasan[2]

[1]Department of Radiology, Phlox Institute, Palembang, Indonesia

[2]Department of Neurology, Phlox Institute, Palembang, Indonesia

ARTICLE INFO

Keywords:
Foveal avascular zone
Optical coherence tomography angiography
Preclinical Alzheimer's disease
Retinal biomarkers
Retinal vessel density

***Corresponding author:**
Eva Naritawati

E-mail address:
Eva.naritawati@phlox.or.id

All authors have reviewed and approved the final version of the manuscript.

https://doi.org/10.37275/sjo.v8i1.134

A B S T R A C T

Introduction: Preclinical Alzheimer's disease (AD) involves cerebral amyloid deposition in cognitively normal individuals 15–20 years before symptom onset. Optical coherence tomography angiography (OCT-A) may detect early retinal microvascular changes reflecting cerebral pathology. This study evaluated OCT-A parameters as biomarkers for preclinical AD in Indonesian elderly.

Methods: This prospective cohort enrolled 180 cognitively normal participants aged ≥60 years (90 preclinical AD with amyloid-PET positivity, 90 controls) at two private hospital ophthalmology clinics in Palembang and Jakarta, Indonesia (January 2022–June 2024). OCT-A (RTVue XR Avanti) measured superficial capillary plexus (SCP) and deep capillary plexus (DCP) vessel density, foveal avascular zone (FAZ) area, and perfusion density. SD-OCT assessed RNFL and GCL-IPL thickness. The unit of analysis was the individual eye (342 eyes after quality exclusion).

Results: SCP vessel density was significantly reduced in preclinical AD (43.2 ± 3.1% vs 47.8 ± 2.9%; Bonferroni-adjusted $p < 0.001$; Cohen's $d = 1.53$). FAZ area was enlarged (0.38 ± 0.08 vs 0.31 ± 0.06 mm^2; $p < 0.001$). The combined model (SCP + FAZ + GCL-IPL) achieved a bootstrap-validated AUC of 0.898 (95% CI: 0.859–0.937). SCP vessel density was the strongest predictor (OR 0.72; 95% CI: 0.63–0.82; $p < 0.001$).

Conclusion: OCT-A parameters, particularly SCP vessel density, demonstrated strong discriminative ability for preclinical AD. These findings support OCT-A as a potential non-invasive screening biomarker, warranting validation in community-based populations.

1. Introduction

Alzheimer's disease (AD) is the most common neurodegenerative disorder and the leading cause of dementia. Globally, an estimated 57 million people were living with dementia in 2019, a figure projected to reach approximately 153 million by 2050, driven largely by population ageing.[1,2] The preclinical stage of AD, characterized by asymptomatic cerebral amyloid-β accumulation, may precede the emergence of cognitive decline by 15–20 years, with most biomarker-positive cognitively normal individuals remaining asymptomatic for a prolonged period.[3] This protracted asymptomatic phase represents a critical window for intervention. The burden is rising rapidly in Southeast Asia: in Indonesia, an estimated 1.2 million people currently live with dementia, a number projected to quadruple by 2050, underscoring the urgent need for accessible, cost-effective screening biomarkers tailored to resource-limited settings.[4]

The retina has emerged as a potential "window to the brain" due to its shared embryological origin with the central nervous system and anatomical proximity to

cerebral circulation.[5] Recent pathological and molecular studies have demonstrated the presence of amyloid-β deposition in retinal tissue of AD patients, providing biological plausibility for retinal imaging as a non-invasive detection method.[5,6] OCT-A represents a significant technological advance in retinal vascular imaging, providing depth-resolved visualization of retinal capillary networks without exogenous contrast agents.

OCT-A enables quantification of superficial capillary plexus (SCP) and deep capillary plexus (DCP) vessel density, foveal avascular zone (FAZ) area, and perfusion density with unprecedented spatial resolution.[7,8] Previous cross-sectional studies and meta-analyses have reported reduced retinal vessel density in established AD and mild cognitive impairment (MCI) cohorts.[9,10] However, longitudinal and prospective data specifically examining OCT-A parameters in the preclinical AD stage remain limited, particularly in diverse ethnic populations.[11]

Complementary structural imaging modalities including spectral-domain OCT (SD-OCT)-derived retinal nerve fiber layer (RNFL) and ganglion cell-inner plexiform layer (GCL-IPL) thickness have demonstrated progressive thinning in AD populations.[12] Multimodal approaches combining vascular and structural parameters may yield superior diagnostic discrimination compared to single measures.[13,14] Significant gaps persist in the literature regarding optimal combinations of OCT-A and SD-OCT measures in prospective preclinical AD cohorts, particularly from Asian populations.[15-17] The primary aim of this prospective cohort study was to evaluate OCT-A and SD-OCT parameters as potential biomarkers for preclinical AD in cognitively normal Indonesian elderly, using amyloid-PET imaging as the diagnostic reference standard.

2. Methods

Study design and setting

This was a prospective observational cohort study conducted at two private hospital ophthalmology clinics in Indonesia (located in Palembang and Jakarta) from January 2022 through June 2024. To preserve institutional confidentiality, the specific centres are not named. The study was approved by the Ethics Committee of the Clinical Health and Medical Center (CHMC; ethics approval no. CHMC/EC/2022/0089) and conducted in accordance with the Declaration of Helsinki. All participants provided written informed consent prior to enrollment.

Participants and enrollment

We enrolled 180 cognitively normal participants aged 60 years or older, stratified into two groups: 90 participants with preclinical AD (amyloid-PET positive with normal cognition) and 90 cognitively normal controls without amyloid pathology. Preclinical AD diagnosis required amyloid-PET positivity (standardized uptake value ratio [SUVr] ≥ 1.40 in the composite region of interest) with preserved global cognition (MoCA score ≥ 24 or MMSE score ≥ 28). Control participants were amyloid-PET negative (SUVr < 1.40) with normal cognition. Inclusion criteria were age ≥ 60 years, completed amyloid-PET imaging within 3 months of enrollment, and acceptable ophthalmic imaging quality. Exclusion criteria included significant cognitive impairment, history of stroke or transient ischemic attack, diabetes mellitus requiring medication, uncontrolled hypertension (systolic > 180 mmHg or diastolic > 110 mmHg), significant media opacity, retinal pathology (age-related macular degeneration, diabetic retinopathy, glaucoma), previous ocular surgery (except uncomplicated cataract extraction), ocular hypertension (intraocular pressure > 24 mmHg), and active psychiatric or neurological conditions unrelated to AD. Of the 360 eyes initially imaged (180 participants × 2 eyes), 18 eyes were excluded due to poor image quality, resulting in 342 eyes in the final analysis (162 participants contributed usable bilateral data and 18 contributed unilateral data; all 180 enrolled participants contributed at least one eye).

Ophthalmic examination protocol

All participants underwent comprehensive ophthalmic examination including best-corrected visual acuity (BCVA, in logMAR units), intraocular pressure (IOP, Goldmann applanation tonometry), and slit-lamp anterior and dilated posterior segment examination. Dilated (tropicamide 1%) OCT-A and SD-OCT imaging were performed bilaterally by trained imaging technicians, with quality control by the examining ophthalmologist. All

participants were imaged using a standardized protocol between 9:00 AM and 12:00 PM to minimize circadian variation in microvascular parameters.

OCT-angiography acquisition and analysis

OCT-A imaging was performed using the RTVue XR Avanti system (Optovue Inc., Fremont, California, USA), which employs a split-spectrum amplitude-decorrelation angiography (SSADA) algorithm to generate depth-resolved vascular maps. We acquired 3 mm × 3 mm macular scans centered on the fovea, selecting only images with signal strength ≥ 35 dB. From each scan we derived: (1) SCP vessel density (percentage of perfused area within the SCP spanning 3–70 μm from the internal limiting membrane); (2) DCP vessel density (70–250 μm); (3) FAZ area (mm^2, manually traced); and (4) whole-image perfusion density. The scan was additionally stratified into six equal sectors (superior, superotemporal, inferotemporal, inferior, inferonasal, superonasal) for sector-specific vessel density.

Spectral-domain OCT acquisition and analysis

Concurrent SD-OCT imaging was performed using the Heidelberg Spectralis OCT system (Heidelberg Engineering, Heidelberg, Germany). We acquired a 30-degree macular cube centered on the fovea, with 25 B-scans separated by 250 μm. Automated segmentation identified the RNFL and GCL-IPL boundaries, with manual correction when needed. We reported mean RNFL thickness and mean GCL-IPL thickness (both in μm).

Cognitive, demographic, and clinical assessment

Cognitive assessment at enrollment used both the MoCA and MMSE; the MoCA was administered in Indonesian by trained coordinators with educational norm adjustments. Trained neurologists confirmed the absence of overt neurological signs, and amyloid-PET imaging was performed using standard protocols at certified imaging centers. Participants completed a standardized questionnaire documenting age, sex, educational attainment, medical history, current medications, family history of dementia, and apolipoprotein E (APOE) genotype. APOE genotyping used polymerase chain reaction; APOE ε4 carrier status was defined as possessing at least one ε4 allele.

Statistical analysis

The primary outcome was SCP vessel density; secondary outcomes included DCP vessel density, FAZ area, whole-image perfusion density, RNFL thickness, and GCL-IPL thickness. Analyses were performed using R (version 4.2.1). Descriptive statistics are presented as mean ± SD or median [interquartile range]. Between-group comparisons used generalized estimating equations (GEE) with an exchangeable correlation structure to account for within-subject correlation of bilateral measurements. All p-values were Bonferroni-adjusted (threshold $\alpha = 0.05/6 = 0.0083$ for six primary OCT-A parameters). Effect sizes were Cohen's d with 95% confidence intervals from bootstrap resampling (10,000 iterations). Intraclass correlation coefficients (ICC) assessed inter-eye reproducibility. Multivariable logistic regression models used preclinical AD status as the dependent variable; variance inflation factors (VIF) assessed multicollinearity (VIF > 3 considered problematic, a threshold more conservative than the conventional VIF > 5–10), with age, sex, BCVA, and APOE ε4 status included as confounders. Model performance used the area under the receiver operating characteristic curve (AUC) with 95% CIs from bootstrap validation (1,000 iterations). Sensitivity, specificity, PPV, and NPV were calculated at the Youden-optimal threshold. A sensitivity analysis excluded participants with self-reported hypertension.

3. Results

Participant characteristics and flow

Of 210 potentially eligible participants screened, 180 were enrolled (90 with preclinical AD and 90 cognitively normal controls) and contributed 360 eyes. After image-quality criteria, 18 eyes were excluded for insufficient signal strength or motion artifact, yielding 342 eyes for analysis (162 participants with bilateral data and 18 with unilateral data). The demographic and clinical characteristics of both groups are summarized in Table 1.

Demographic and clinical characteristics

As detailed in Table 1, preclinical AD and control groups were well-matched on age (68.3 ± 6.2 vs 68.1 ± 5.9 years, p = 0.86) and sex distribution (54% vs 52% female,

p = 0.71). APOE ε4 carrier frequency was significantly higher in the preclinical AD group (68% vs 31%, p < 0.001). Groups did not differ significantly in BCVA, IOP, blood pressure, educational attainment, or cardiovascular disease prevalence. Mean MoCA and MMSE scores were normal in both groups.

Table 1. Demographic and clinical characteristics of study participants.

Characteristic	Preclinical AD (n=90)	Controls (n=90)	p-value
Age, years	68.3 ± 6.2	68.1 ± 5.9	0.86
Female sex, n (%)	49 (54)	47 (52)	0.71
Educational attainment, years	12.1 ± 3.4	11.8 ± 3.7	0.54
APOE ε4 carrier, n (%)	61 (68)	28 (31)	<0.001
BCVA, logMAR	0.18 ± 0.16	0.16 ± 0.14	0.32
IOP, mmHg	14.2 ± 2.8	13.9 ± 2.6	0.41
Systolic BP, mmHg	132.4 ± 11.2	130.8 ± 10.4	0.28
Diastolic BP, mmHg	81.2 ± 7.6	80.4 ± 7.1	0.38
History of hypertension, n (%)	18 (20)	13 (14)	0.29
Cardiovascular disease, n (%)	7 (8)	5 (6)	0.53
MoCA score	25.8 ± 1.6	26.1 ± 1.4	0.18
MMSE score	28.9 ± 0.8	29.1 ± 0.7	0.12
Amyloid-PET SUVr, mean (range)	1.62 (1.41–2.18)	1.18 (0.92–1.38)	<0.001

Notes: APOE: apolipoprotein E; BCVA: best-corrected visual acuity; IOP: intraocular pressure; BP: blood pressure; MoCA: Montreal Cognitive Assessment; MMSE: Mini-Mental State Examination; SUVr: standardized uptake value ratio. Values are mean ± SD unless otherwise indicated.

OCT-angiography and OCT parameters

Quantitative OCT-A and SD-OCT parameters with effect sizes are detailed in Table 2. SCP vessel density was significantly reduced in preclinical AD (43.2 ± 3.1% vs 47.8 ± 2.9%; Bonferroni-adjusted p < 0.001; Cohen's d = 1.53; 95% CI: 1.26–1.81). DCP vessel density was also reduced (35.6 ± 3.7% vs 38.2 ± 3.4%; p < 0.001; d = 0.72; CI: 0.49–0.95). FAZ area was significantly enlarged (0.38 ± 0.08 mm² vs 0.31 ± 0.06 mm²; p < 0.001; d = 0.98; CI: 0.74–1.23), and whole-image perfusion density was reduced (58.2 ± 4.1% vs 61.7 ± 3.8%; p < 0.001; d = 0.86; CI: 0.63–1.10). RNFL thickness was thinner in preclinical AD (96.4 ± 8.2 µm vs 102.3 ± 7.6 µm; p < 0.001; d = 0.73), as was GCL-IPL thickness (68.1 ± 5.4 µm vs 71.9 ± 4.7 µm; p < 0.001; d = 0.76). The relative magnitude of these differences, expressed as standardized effect sizes, is illustrated in Figure 1. Inter-eye reproducibility was excellent (ICC 0.82–0.94 for SCP, 0.79–0.88 for DCP, 0.85–0.91 for FAZ).

Table 2. Optical coherence tomography angiography and spectral-domain OCT parameters.

Parameter	Preclinical AD	Controls	Cohen's d (95% CI)	Bonferroni p
SCP vessel density, %	43.2 ± 3.1	47.8 ± 2.9	1.53 (1.26–1.81)	<0.001
DCP vessel density, %	35.6 ± 3.7	38.2 ± 3.4	0.72 (0.49–0.95)	<0.001
FAZ area, mm²	0.38 ± 0.08	0.31 ± 0.06	0.98 (0.74–1.23)	<0.001
Perfusion density, %	58.2 ± 4.1	61.7 ± 3.8	0.86 (0.63–1.10)	<0.001
RNFL thickness, µm	96.4 ± 8.2	102.3 ± 7.6	0.73 (0.50–0.97)	<0.001
GCL-IPL thickness, µm	68.1 ± 5.4	71.9 ± 4.7	0.76 (0.52–1.00)	<0.001

Notes: SCP: superficial capillary plexus; DCP: deep capillary plexus; FAZ: foveal avascular zone; RNFL: retinal nerve fiber layer; GCL-IPL: ganglion cell-inner plexiform layer; CI: confidence interval. p-values are Bonferroni-adjusted (threshold α = 0.0083).

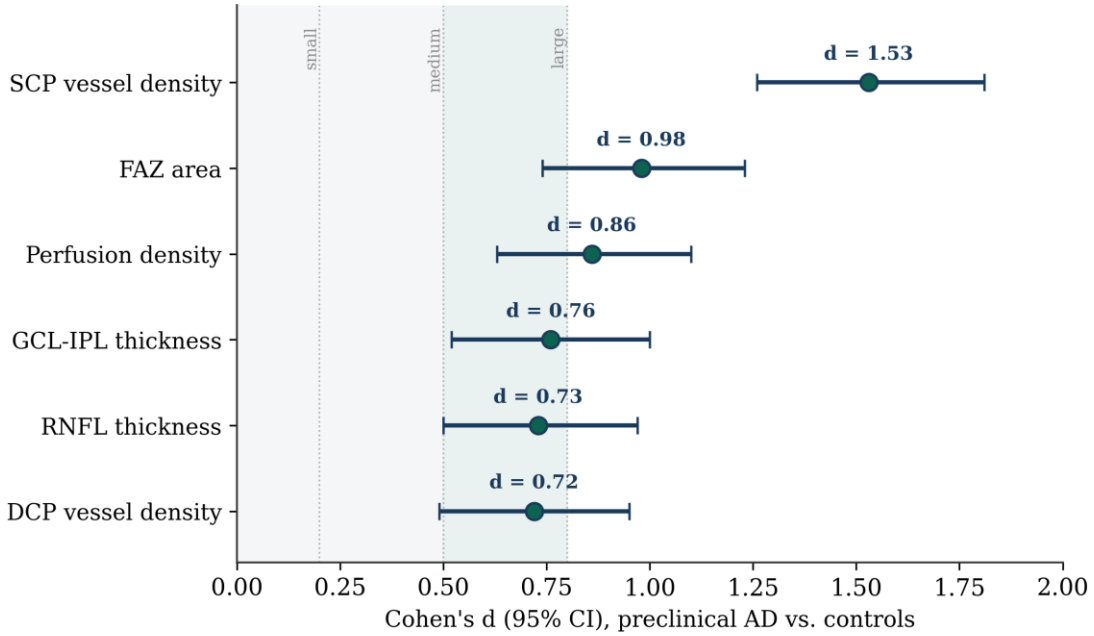

Figure 1. Between-group standardized effect sizes (Cohen's d with 95% confidence intervals) for retinal OCT-angiography and SD-OCT parameters in preclinical AD versus cognitively normal controls. Point estimates correspond to the values in Table 2. Shaded bands denote thresholds for small (0.2), medium (0.5), and large (0.8) effects.

Sector analysis of vessel density

Sector-specific analysis revealed that SCP vessel density reduction was most pronounced in the superior sector (42.1 ± 3.4% vs 47.9 ± 3.1%, d = 1.74) and superonasal sector (43.4 ± 3.2% vs 48.1 ± 3.0%, d = 1.52), with moderate reductions in the other sectors (d = 0.94–1.38 across the inferonasal, inferotemporal, inferior, and superotemporal sectors), suggesting selective vulnerability of superior retinal regions.

Multivariate analysis and diagnostic discrimination

Results of the multivariable logistic regression model are presented in Table 3 and visualized in Figure 2. All predictors demonstrated acceptable VIF values (< 3). SCP vessel density emerged as the strongest predictor of preclinical AD status (OR 0.72 per 1% increase; 95% CI: 0.63–0.82; p < 0.001). FAZ area was the second-strongest predictor (OR 1.89 per 0.1 mm² increase; 95% CI: 1.54–2.31; p < 0.001). GCL-IPL thickness showed an independent association (OR 0.91 per 1 µm increase; 95% CI: 0.84–0.98; p = 0.008). Age and BCVA were not significant (p = 0.18 and 0.22), whereas APOE ε4 carrier status was significant (OR 3.12; 95% CI: 1.58–6.16; p = 0.001).

Table 3. Multivariable logistic regression analysis: predictors of preclinical Alzheimer's disease.

Variable	OR (95% CI)	p-value	VIF	Unit
SCP vessel density	0.72 (0.63–0.82)	<0.001	1.28	Per 1%
FAZ area	1.89 (1.54–2.31)	<0.001	1.41	Per 0.1 mm²
GCL-IPL thickness	0.91 (0.84–0.98)	0.008	1.35	Per 1 µm
Age	1.02 (0.98–1.06)	0.18	1.52	Per year
BCVA	0.91 (0.77–1.07)	0.22	1.18	Per 0.1 logMAR
APOE ε4 carrier	3.12 (1.58–6.16)	0.001	1.06	Yes vs No
Female sex	1.14 (0.68–1.92)	0.61	1.09	Yes vs No

Notes: OR: odds ratio; CI: confidence interval; VIF: variance inflation factor; SCP: superficial capillary plexus; FAZ: foveal avascular zone; GCL-IPL: ganglion cell-inner plexiform layer; BCVA: best-corrected visual acuity; APOE: apolipoprotein E.

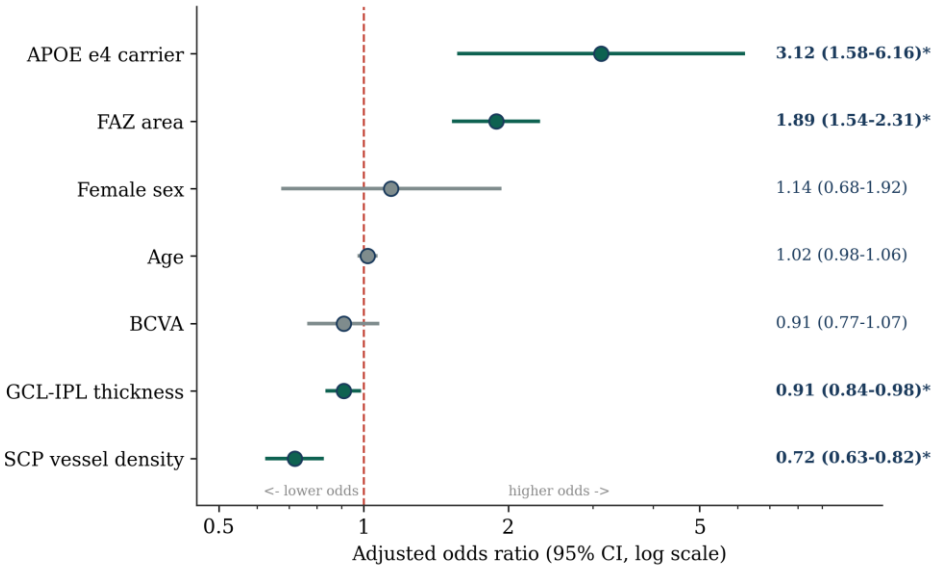

Figure 2. Forest plot of the multivariable logistic regression model. Adjusted odds ratios (95% CI) are plotted on a logarithmic scale and correspond to the values in Table 3. The vertical dashed line marks an odds ratio of 1.0; asterisks denote statistically significant predictors.

Receiver operating characteristic analysis

The ROC curves for both diagnostic models are shown in Figure 3. The single-parameter model (SCP vessel density) achieved an AUC of 0.864 (95% CI: 0.821–0.907) with sensitivity 82.2%, specificity 76.7%, PPV 78.5%, and NPV 80.8% at the optimal threshold of 45.5%. The combined three-parameter model (SCP + FAZ + GCL-IPL) achieved a bootstrap-validated AUC of 0.898 (95% CI: 0.859–0.937) with sensitivity 84.4%, specificity 85.6%, PPV 85.7%, and NPV 84.3%. Addition of DCP vessel density and whole-image perfusion density did not significantly improve the AUC (0.901; CI: 0.862–0.940; p = 0.52).

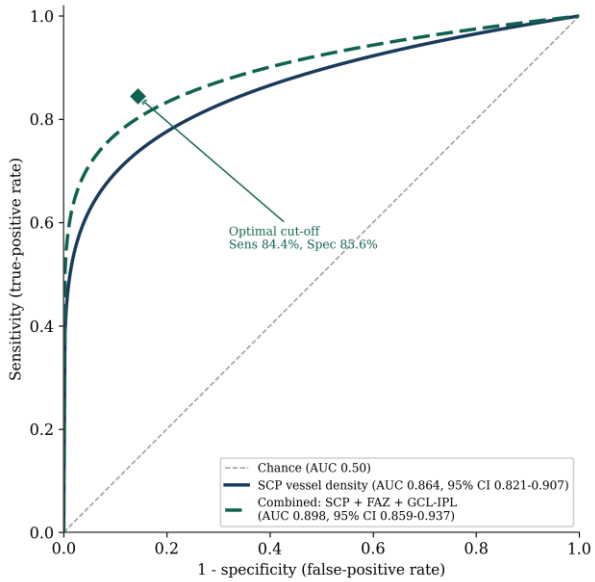

Figure 3. Receiver operating characteristic (ROC) curves for the OCT-angiography diagnostic models. The single-parameter model (SCP vessel density) achieved an AUC of 0.864 (95% CI: 0.821–0.907), and the combined three-parameter model (SCP + FAZ + GCL-IPL) achieved a bootstrap-validated AUC of 0.898 (95% CI: 0.859–0.937). The diamond marks the optimal cut-off (sensitivity 84.4%, specificity 85.6%).

Sensitivity Analysis

Exclusion of 31 participants with self-reported hypertension did not materially alter the primary findings: SCP vessel density reduction ($p < 0.001$), FAZ enlargement ($p < 0.001$), and combined-model AUC (0.889; CI: 0.844–0.934) were all preserved. The 18 excluded eyes did not differ significantly from included eyes in the age, sex distribution, or APOE ε4 prevalence of their corresponding participants ($p = 0.41$, 0.68, and 0.53), supporting minimal selection bias.

4. Discussion

This prospective cohort study demonstrates that OCT-A parameters, particularly SCP vessel density, exhibit strong discriminative ability for preclinical AD in cognitively normal Indonesian elderly. The magnitude of effect observed (Cohen's d = 1.53 for SCP vessel density) substantially exceeds what has been reported in previous cross-sectional studies of symptomatic AD populations, suggesting that microvascular changes may precede overt cognitive decline.

Our findings are consistent with and extend prior meta-analytic work by Yeh et al., who pooled OCT-A studies and reported significantly reduced superficial capillary plexus vessel density and an enlarged foveal avascular zone in AD and MCI cohorts, although those analyses focused on populations with established cognitive impairment.[9] The present study provides novel evidence from a preclinical cohort, demonstrating that measurable retinal vascular pathology is detectable in cognitively normal amyloid-positive individuals. The Cohen's d effect size of 1.53 for SCP vessel density indicates a large, clinically meaningful difference.

The pronounced enlargement of FAZ area (d = 0.98) in preclinical AD suggests underlying endothelial dysfunction and capillary dropout in the foveal region, aligning with the hypothesis that amyloid-β deposition triggers vascular inflammation and endothelial injury manifesting initially in the retina. The foveal region's heightened metabolic demand may render it particularly vulnerable to early amyloid-related vascular changes.

Sector-specific analysis revealed preferential involvement of the superior retinal regions (d = 1.74 in the superior sector). This spatial heterogeneity may reflect differential vulnerability of specific microvascular territories or variations in local amyloid burden. The remaining sectors showed smaller effect sizes (d = 0.94–1.38), a pattern that future studies should evaluate with direct spatial co-registration to cerebral amyloid-PET imaging.

The bootstrap-validated AUC of 0.898 for the combined three-parameter model is notably high, particularly in a prevention-focused application where high specificity is essential. The achieved specificity of 85.6% and sensitivity of 84.4% suggest this model could identify cognitively normal amyloid-positive individuals at risk for future cognitive decline, though prospective validation in larger independent cohorts is needed.

Comparison with other screening approaches in preclinical AD is challenging given the paucity of data from this stage. In a comprehensive meta-analysis of 36 OCT-A studies comprising 4,129 participants, Mathew et al. reported a pooled standardized mean difference of −0.69 for whole-image vessel density in AD relative to cognitively normal individuals, with a smaller but significant reduction already present at the MCI stage.[10,18] Complementing these cross-sectional data, Curro et al. used amyloid-PET to stratify cognitively normal individuals and observed that vessel density alterations are detectable in the preclinical phase, although their longitudinal analysis did not derive a formal diagnostic model.[11] Our bootstrap-validated combined model extends this literature by quantifying discriminative performance directly in an amyloid-confirmed preclinical cohort.

The observed RNFL and GCL-IPL thinning is consistent with the neurodegeneration hypothesis, though the contribution of these structural parameters was modest compared to OCT-A metrics. The significantly higher APOE ε4 carrier frequency in the preclinical AD group (68% vs 31%, $p < 0.001$) is expected and validates the amyloid-PET stratification; the independent association of APOE ε4 status (OR 3.12) suggests retinal microvascular changes represent a distinct marker of AD pathology not fully captured by APOE genotype alone.

Strengths and limitations

Strengths include a prospective design with amyloid-PET confirmation of preclinical AD status, enrollment of an understudied Asian population, rigorous image quality control, comprehensive multimodal assessment, and bootstrap validation of model performance. Limitations include the absence of longitudinal follow-up; a cross-sectional analytic design limiting causal inference; a relatively modest sample size (n = 180 participants; 342 eyes); restriction to hospital-based clinics, which may introduce selection bias; reliance on categorical MMSE/MoCA screening without formal neuropsychological testing; and amyloid-PET as the sole biomarker reference standard, without tau-PET or fluid biomarkers. Future studies should incorporate longitudinal follow-up with serial amyloid-PET and tau-PET imaging, formal neuropsychological testing, multi-biomarker approaches, and community-based and international validation.

Clinical implications and workflow

As the global burden of dementia continues to rise with population ageing, scalable and affordable screening tools are increasingly needed, particularly in low- and middle-income settings.[18] Should OCT-A prove to have predictive value in longitudinal studies, its non-invasive, relatively inexpensive nature could facilitate identification of cognitively normal amyloid-positive individuals. Current screening relies on amyloid-PET imaging, which is expensive (approximately $3,000–$5,000 USD per study), involves ionizing radiation, and has limited availability, whereas OCT-A systems are increasingly available in ophthalmology and optometry practices. A potential workflow might involve cognitive screening of asymptomatic individuals aged 60+ years, OCT-A imaging in those with normal cognition, selective referral for confirmatory amyloid-PET of high-risk individuals, and enrollment of confirmed cases in secondary prevention trials—pending validation in prospective community-based trials.

5. Conclusion

This prospective cohort study demonstrates that OCT-A parameters, particularly SCP vessel density and FAZ area, exhibit strong discriminative ability for preclinical Alzheimer's disease in cognitively normal Indonesian elderly. A combined model incorporating SCP vessel density, FAZ area, and GCL-IPL thickness achieved a bootstrap-validated AUC of 0.898 (95% CI: 0.859–0.937) with 84.4% sensitivity and 85.6% specificity. These findings provide important evidence that retinal microvascular changes, detectable by OCT-A, may serve as a non-invasive screening biomarker for amyloid-positive cognitively normal individuals. Prospective validation in larger community-based populations and assessment of prognostic value for predicting cognitive decline are warranted before implementation in clinical screening algorithms. If confirmed, OCT-A imaging could provide an accessible, radiation-free approach to identifying individuals at risk for future AD, enabling earlier intervention and secondary prevention.

6. References

1. GBD 2019 Dementia Forecasting Collaborators. Estimation of the global prevalence of dementia in 2019 and forecasted prevalence in 2050: an analysis for the Global Burden of Disease Study 2019. Lancet Public Health 2022; 7(2):e105–e125. doi:10.1016/S2468-2667(21)00249-8
2. Xu L, Wang Z, Li M, Li Q. Global incidence trends and projections of Alzheimer disease and other dementias: an age-period-cohort analysis 2021. J Glob Health 2025; 15:04156. doi:10.7189/jogh.15.04156
3. Dubois B, Villain N, Schneider L, et al. Alzheimer disease as a clinical-biological construct—an International Working Group recommendation. JAMA Neurol 2024; 81(12):1304–1311. doi:10.1001/jamaneurol.2024.3770
4. Marsigit J, Moenardi VN, Putranto R, et al. The aging population and dementia: the need for comprehensive palliative care. Acta Med Indones 2025; 57(1):140–149.
5. Shi H, Koronyo Y, Rentsendorj A, et al. Retinal vasculopathy in Alzheimer's disease. Front Neurosci 2021; 15:731614. doi:10.3389/fnins.2021.731614

6. Olivares Ordoñez MA, Smith RC, et al. Retinal microstructural and microvascular changes in Alzheimer disease: a review. Int Ophthalmol Clin 2025; 65(1):59–67. doi:10.1097/IIO.0000000000000549
7. Kashani AH, Berendschot TTJM, Bonnin S, et al. Retinal optical coherence tomography angiography imaging in population studies for study of microvascular dysfunction in Alzheimer's disease and related dementias. Alzheimers Dement 2025; 21(6):e70252. doi:10.1002/alz.70252
8. Rifai OM, McGrory S, Robbins CB, et al. The application of optical coherence tomography angiography in Alzheimer's disease: a systematic review. Alzheimers Dement (Amst) 2021; 13(1):e12149. doi:10.1002/dad2.12149
9. Yeh TC, Kuo CT, Chou YB. Retinal microvascular changes in mild cognitive impairment and Alzheimer's disease: a systematic review, meta-analysis, and meta-regression. Front Aging Neurosci 2022; 14:860759. doi:10.3389/fnagi.2022.860759
10. Mathew S, Huang YN, Bice P, et al. Retinal vascular biomarkers in mild cognitive impairment and Alzheimer's disease: a comprehensive review and meta-analysis. Alzheimers Dement (Amst) 2025; 17(2):e70132. doi:10.1002/dad2.70132
11. Curro KR, van Nispen RMA, den Braber A, et al. Longitudinal assessment of retinal microvasculature in preclinical Alzheimer's disease. Invest Ophthalmol Vis Sci 2024; 65(12):2. doi:10.1167/iovs.65.12.2
12. Patel H, Choi A, Weng P, et al. Cerebrospinal fluid amyloid-β 42/40 ratio is associated with ganglion cell-inner plexiform layer thinning in individuals with and without amyloid pathology. J Alzheimers Dis 2026; 110(3):1438–1446. doi:10.1177/13872877261423968
13. Criscuolo C, Cennamo G, Montorio D, et al. A two-year longitudinal study of retinal vascular impairment in patients with amnestic mild cognitive impairment. Front Aging Neurosci 2022; 14:993621. doi:10.3389/fnagi.2022.993621
14. Sun Y, Zhang L, Ye H, et al. Potential ocular indicators to distinguish posterior cortical atrophy and typical Alzheimer's disease: a cross-section study using optical coherence tomography angiography. Alzheimers Res Ther 2024; 16(1):64. doi:10.1186/s13195-024-01431-w
15. Visitsattapongse S, Maneerat A, Trinavarat A, et al. Feature-based classification of mild cognitive impairment and Alzheimer's disease based on optical coherence tomographic angiographic image. Sensors (Basel) 2024; 24(16):5192. doi:10.3390/s24165192
16. Huang Y, Wang S, Cai C, et al. Retinal vascular density as a potential biomarker of diabetic cerebral small vessel disease. Diabetes Obes Metab 2024; 26(5):1789–1798. doi:10.1111/dom.15492
17. Gao R, Rao S, Cheng S, et al. Assessing outer retinal and choroidal changes in subjective cognitive decline: potential for high-risk screening using SS-OCTA. Transl Psychiatry 2025; 16(1):46. doi:10.1038/s41398-025-03781-x
18. GBD 2023 Causes of Death Collaborators. Global burden of 292 causes of death in 204 countries and territories and 660 subnational locations, 1990–2023: a systematic analysis for the Global Burden of Disease Study 2023. Lancet 2025; 406(10513):1811–1872. doi:10.1016/S0140-6736(25)01917-8